Landscape Ecol
DOI 10.1007/s10980-012-9723-6

RESEARCH ARTICLE

Forest fragmentation, climate change and understory fire regimes on the Amazonian landscapes of the Xingu headwaters

Britaldo Soares-Filho · Rafaella Silvestrini · Daniel Nepstad · Paulo Brando · Hermann Rodrigues · Ane Alencar · Michael Coe · Charton Locks · Letícia Lima · Letícia Hissa · Claudia Stickler

Received: 14 February 2011 / Accepted: 6 February 2012

Abstract Understory fire modeling is a key tool to investigate the cornerstone concept of landscape ecology, i.e. how ecological processes relate to landscape structure and dynamics. Within this context, we developed FISC—a model that simulates fire ignition and spread and its effects on the forest carbon balance. FISC is dynamically coupled to a land-use change model to simulate fire regimes on the Amazonian landscapes of the Xingu Headwaters under deforestation, climate change, and land-use management scenarios. FISC incorporates a stochastic cellular automata approach to simulate fire spread across agricultural and forested lands. CARLUC, nested in FISC, simulates fuel dynamics, forest regrowth, and carbon emissions. Simulations of fire regimes under modeled scenarios revealed that the major current and future driver of understory fires is forest fragmentation rather than climate change. Fire intensity proved closely related to the landscape structure of the remaining forest. While climate change may increase the percentage of forest burned outside protected areas

Electronic supplementary material The online version of this article (doi:10.1007/s10980-012-9723-6) contains supplementary material, which is available to authorized users.

B. Soares-Filho (✉) · R. Silvestrini · H. Rodrigues · L. Lima · L. Hissa
Centro de Sensoriamento Remoto, Universidade Federal de Minas Gerais, Av. Antônio Carlos, 6627, Belo Horizonte, MG 31270-900, Brazil
e-mail: britaldo@csr.ufmg.br

R. Silvestrini
e-mail: rafaella@csr.ufmg.br

H. Rodrigues
e-mail: hermann@csr.ufmg.br

L. Lima
e-mail: leticialima@csr.ufmg.br

L. Hissa
e-mail: leticiaviana@csr.ufmg.br

D. Nepstad · P. Brando · A. Alencar · C. Stickler
Instituto de Pesquisa Ambiental da Amazônia – IPAM, Av. Nazaré 669, Belém, PA 66035-170, Brazil
e-mail: dnepstad@ipam.org.br

P. Brando
e-mail: pmbrando@ipam.org.br

A. Alencar
e-mail: ane@ipam.org.br

C. Stickler
e-mail: cstickler@ipam.org

M. Coe
The Woods Hole Research Center, 149 Woods Hole Road, Falmouth, MA 02540-1644, USA
e-mail: mtcoe@whrc.org

C. Locks
Aliança da Terra, Av. das Indústrias 601, Qd 151–Lt 47–Sala 203, Goiânia, GO 74670-600, Brazil
e-mail: chartonjlocks@gmail.com

Published online: 15 March 2012

by 30% over the next four decades, deforestation alone may double it. Nevertheless, a scenario of forest recovery and better land-use management would abate fire intensity by 18% even in the face of climate change. Over this time period, the total carbon balance of the Xingu's forests varies from an average net sink of 1.6 ton ha^{-1} $year^{-1}$ in the absence of climate change, fire and deforestation to a source of −0.1 ton ha^{-1} $year^{-1}$ in a scenario that incorporates these three processes.

Keywords Carbon fluxes · Landscape dynamics · Landscape metrics · Spatially-explicit modeling · Land-use management

Introduction

Interactions between deforestation and climate drive the frequency and magnitude of wildfires in the Amazon (Nepstad et al. 1999; Cochrane 2003). During the 1997–1998 El Niño event, about 10,000 km^2 of forests burned in the state of Roraima in the northern Amazon (Phulpin et al. 2002) and in 2005, the unusual warming of tropical North Atlantic waters resulted in a threefold increase in the number of fires in the southwestern Amazon (Marengo et al. 2008). In addition to the direct consequences of fire for forest ecosystems, there is a growing concern about the potential effects of wildfires on global warming, as they affect the carbon balance between the atmosphere and the forest. The Amazon forest contains one-tenth of global carbon stored in land ecosystems and accounts for one-tenth of net primary production worldwide (Melillo et al. 1993). In El Niño years, however, carbon emissions from forest fires in the Brazilian Amazon may reach between 0.024 and 0.165 Pg (Alencar et al. 2006), playing, therefore, an important role in global warming.

In the near future, climate change may increase the frequency of wildfires (Silvestrini et al. 2011), as large parts of the Amazon may become warmer and drier (Oyama and Nobre 2003; Betts et al. 2004) and drought events—such as the ones of 1997–1998, 2005, and 2010—become more frequent due to global warming (Cox et al. 2008). The combined effects of a warmer climate and rainfall reduction, with the latter further aggravated by deforestation (Sampaio et al. 2007), would eventually lead to the substitution of large parts of the Amazon moist forests by a savanna-like vegetation (Oyama and Nobre 2003; Nepstad et al. 2008), thereby increasing the susceptibility of remaining forests to fire. The degree to which this process will affect the Amazon forest is still uncertain and depends on other joint effects of climate change, such as the potential fertilization of vegetation from higher atmospheric CO_2 concentrations (Ramming et al. 2010), and the degree of resilience of remaining forests. In this way, the preservation of large blocks of undisturbed forests could be the most important factor to help sustain the health of Amazon forest ecosystems, given that large tracts of undisturbed forest may maintain microclimates and contribute to the persistence of tropical, humid forests even in the face of climate change (Cochrane and Barber 2009; Malhi et al. 2009).

Today, forest fragmentation and the use of fire as a land management tool are the major drivers of fire in tropical forests. Forest fragmentation has increased the frequency of large fire events in Amazon frontiers from average intervals of fifteen to five years (Cochrane et al. 1999). Disturbance from logging also contributes to forest fires, as it opens the canopy and increases light penetration that dries dead leaves on the floor, thereby decreasing understory humidity and increasing fuel loads and forest flammability (Cochrane 2003). It is common to use fire to restore pasture productivity and to clear forested land for agriculture in the Amazon, and these activities are the major ignition sources for understory fires (Nepstad et al. 1999; Alencar et al. 2004). In these mixed agricultural landscapes, forest fragments become highly susceptible to fires that escape from nearby cleared areas, especially due to lower humidity and higher flammability at forest edges (Kapos et al. 1993; Ray et al. 2005). Fire also begets fire; after an understory fire event, tree mortality produces a combination of increased dead organic matter on the forest floor and a more open canopy, thus increasing the chance of fire recurrence (Nepstad et al. 1999).

The potential consequences of forest fires have called into question our limited understanding of the science of fire in the tropics, and underscored the need to develop models of understory fire as tools to assess the impacts of forest fires in the face of a changing environment due to global warming and increasing anthropogenic forest disturbance. Moreover, fire modeling represents a unique opportunity to investigate the cornerstone concept of landscape ecology, i.e. how landscape function interacts with its spatial pattern over time (Forman and Godron 1986).

Although various studies sought to disentangle the effects of landscape attributes on the process of fire (e.g. Green 1983; Turner and Romme 1994; Johnstone et al. 2011), modeling fire in tropical forests is still at an early stage (Silvestrini et al. 2011). There are only few models of fire for the Amazon, and all of them attempt to describe the risk of fire rather than fire behavior. (e.g. Cardoso et al. 2003; Nepstad et al. 2004; Sismanoglu and Setzer 2005; Silvestrini et al. 2011). All these models were developed by analyzing the space-time distribution of hot pixels, which mostly represent fires in open areas (Silvestrini et al. 2011). Alencar et al. (2004) were the first to evaluate the risk of understory fires in the Amazon by relating forest fire scars mapped from Landsat imagery to forest fragmentation and climatic conditions to predict the probability of forest fires. However, a need exists for a model that integrates current knowledge on both ignition and propagation processes of tropical understory fires. To fill this gap, we developed a process-based understory fire model, FISC (fire ignition, spread and carbon components), and applied it to simulate current and future understory fire regimes and the associated carbon balance of forested landscapes of the Xingu Headwaters under a set of land-cover change, land-use management, and climate change scenarios.

Study region

The Xingu headwaters are located in the southeastern Brazilian Amazon between 9° and 15° south latitude and 51° and 56° west longitude. This dynamic agricultural region comprises a mosaic of large cattle ranches and soybean farms amid large fragments of rainforest, transitional forest, and native savanna—*cerrado* (Stickler et al. 2009). These mixed agricultural and forested landscapes surround the Xingu Indigenous Park, which together with the Capoto-Jarima, Naruv'tu and Wawi reservations, forms a territory of approximately 34,000 km^2 that is home to 18 indigenous groups (Figs. 1 and S1 in Supplementary Material). Of particular importance, the Xingu headwaters house one of the most threatened Amazonian ecosystems due to its fertile soils and close

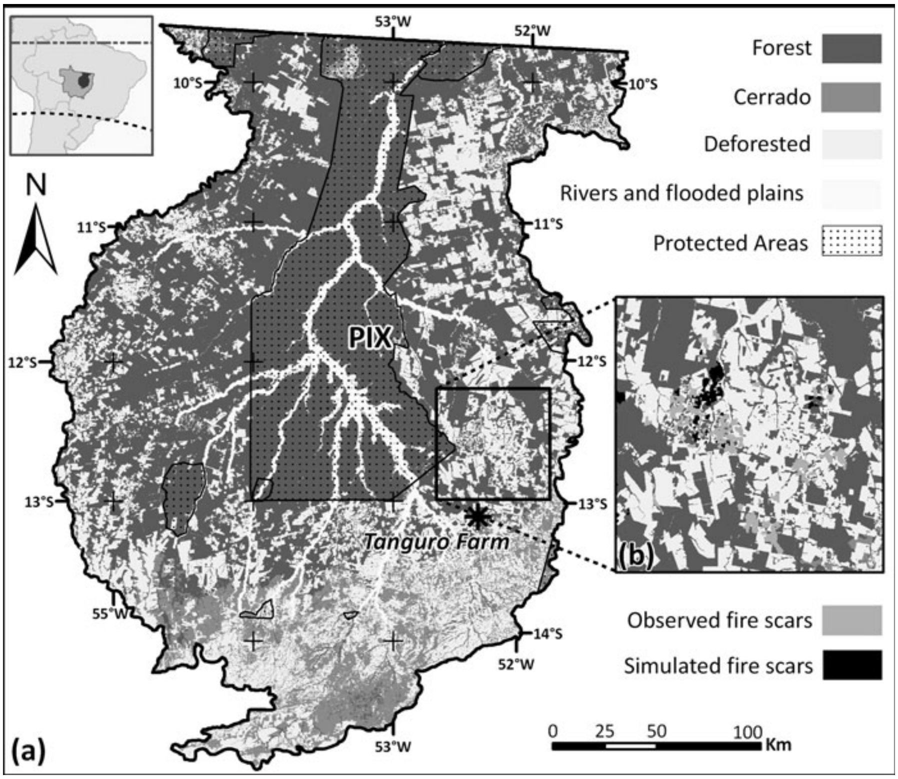

Fig. 1 (*a*) The Xingu Headwaters and its location in Mato Grosso. Tanguro Farm, where fire experiments are being conducted, is pinpointed on the map. PIX stands for the Xingu Indigenous Park. (*b*) Enlarged view of the southern region showing simulated and observed fire scars between January and August 2005

proximity to major population centers, paved roads, and the highly productive grain crop belt in the State of Mato Grosso (Soares-Filho et al. 2006). Our study area covers 176,000 km^2, of which 75,000 and 35,000 km^2 currently consist of forest remnants outside and inside protected areas (PAs), respectively.

Methods

FISC simulates fire ignition and spread and the effects of fire on carbon fluxes between forest pools and from the forest to the atmosphere. FISC incorporates a stochastic CA (cellular automata) approach to simulate fire behavior across agricultural and forested lands. Climatic conditions affect the risk of fire ignition and forest flammability as well as the resilience of the forest following a fire event. The carbon dynamics component of FISC, CARLUC—carbon and land use change (Hirsch et al. 2004) is a spatially-explicit, process-based carbon-cycle model that simulates forest flammability including fuel dynamics, biomass burning, charcoal formation, forest regrowth, and carbon fluxes between forest pools and from the forest to the atmosphere during and after a fire event (Fig. 2). FISC is dynamically coupled to a high spatial resolution, land-cover change model (Stickler et al. 2009; Appendix 1 in Supplementary Material) to simulate fire regimes under a set of scenarios of deforestation, land-use management, and climate change. All modeling and analytical components including a set of selected landscape metrics were implemented using Dinamica EGO freeware (Soares-Filho et al. 2010a).

Data

Fire ignition sources in FISC consist of fire activity maps represented by monthly sums of simulated hot

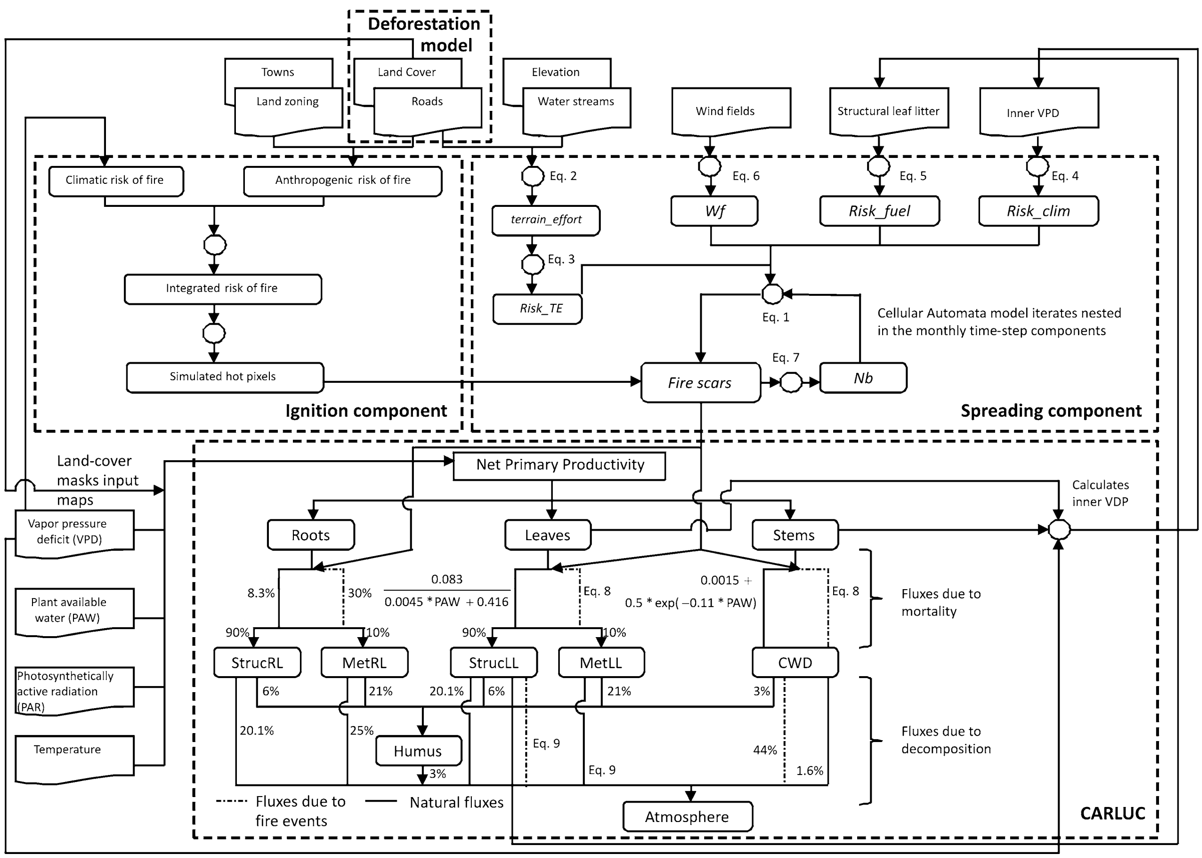

Fig. 2 Flowchart of FISC modules and inputs. Forest carbon pools in CARLUC consist of leaves, stems, roots, structural root litter (*StrucRL*), metabolic root litter (*MetRL*), structural leaf litter (*StrucLL*), metabolic leaf litter (*MetLL*), coarse woody debris (*CWD*) and humus

pixels from a model of fire occurrence (Silvestrini et al. 2011, Appendix 2 in Supplementary Material). To evaluate the spatial association of remotely-sensed hot pixels with fire scars that actually represent understory fires, we derived a map of forest fire scars covering the Xingu headwaters for 2005 by applying the CLAS-BURN algorithm (Alencar et al. 2011) on a mosaic of Landsat-7 TM images acquired on 3 July and 25 August, 2005 (Appendix 3 in Supplementary Material). We concluded that hot pixels that occurred during this same time-period could represent ignition sources for mapped fire scars after testing for spatial association between these events using the K12 function (Appendix 4 in Supplementary Material), whose results confirmed their spatial dependence ($p < 0.05$).

FISC integrates our current knowledge about understory fire behavior obtained from ongoing fire research at Fazenda Tanguro near the southeastern Xingu River (Fig. 1) and previous field measurements (Ray et al. 2005). In this project, 50 ha parcels of forest are burned annually to determine the effects of fire on the state of the forest (Balch et al. 2008). Observations from these experiments were used to establish the effects of fire on fuel dynamics, tree mortality rates, charcoal formation, and biomass burning.

Terrain features incorporated into the model are upslope direction and physical barriers to fire, such as land use and rivers, and wind direction and intensity. Slope was derived from Shuttle Radar Topography Mission maps, and rivers and current land-use come from Stickler et al. (2009). Climate input variables consist of monthly series of temperature, precipitation, plant available water (PAW), photosynthetically active radiation (PAR) and vapor pressure deficit (VPD), all of which were acquired from meteorological stations distributed throughout the Amazon (Hirsch et al. 2004). In addition, CARLUC calculates understory vapor pressure deficit (IVPD) that establishes the degree of forest flammability in FISC (Ray et al. 2005; Balch et al. 2008). Other climate inputs consist of monthly means of wind fields for 2005 obtained from the European Centre for Medium-Range Weather Forecasts (Appendix 5 in Supplementary Material).

Simulated land-cover maps come from Stickler et al. (2009). Cerrado areas in the region were masked in the model for land-cover transitions and carbon balance calculation. To simulate the effects of climate change, we applied the projections from the Had-CM3—Hadley centre coupled model (Cox et al. 1999)—one of the IPCC-AR4 (Intergovernmental Panel on Climate Change, Fourth Assessment Report) general circulation models under the SRES-A2 emission scenario (IPCC 2007). We chose this model because it successfully replicates the effects of El-Niño droughts on Amazon climate (Collins et al 2005; Cox et al. 2008), and thus is widely employed to simulate climate change over the Amazon (e.g. Cox et al. 2004; World Bank 2010). The SRES-A2 scenario is currently considered highly plausible given the constant increase in anthropogenic carbon emissions (Van der Werf et al. 2009), and has been applied to evaluate the likelihood of Amazon dieback (e.g. World Bank 2010).

FISC model

FISC incorporates three components of the fire process: ignition, spread/extinguishment, and the impacts of fire on the state of the forest. The ignition component of FISC is described in Silvestrini et al. (2011). This model integrates the effects of a series of anthropogenic factors—e.g. land-use zoning and proximity to roads, towns and deforested areas—with climatic conditions described by monthly VPD to simulate the occurrence of hot pixels in the Amazon. We recalibrated this model component to run at FISC spatial resolution of 320×320 m (Appendix 2 in Supplementary Material). Any hot pixel that occurs in the forest and within 4 km from its edge is considered to be a potential ignition source for understory fire. Once ignition occurs, fire may run toward and across the forest if a series of environmental conditions are met. These conditions are integrated in a CA model that runs nested within the monthly fire components, as follows:

$$\mathrm{Pburn}_{xy,i,t} = \mathrm{Risk\_TE}_{xy,i} * \mathrm{Risk\_clim}_{xy,i} * \mathrm{Risk\_fuel}_{xy,i} * \mathrm{Wf}_{xy,i,t} * \mathrm{Nbf}_{xy,i,t} \quad (1)$$

where $\mathrm{Pburn}_{xy,\ i,\ t}$ is the probability that a cell with location x, y will catch fire in month i and CA time step t, and Risk_TE is the probability of fire propagation due to landscape features. Monthly climate conditions are incorporated through the climatic risk of fire Risk_Clim and Risk_Fuel, which is the probability that fire will spread as a function of fuel loads. In the CA, the combined probability of these three components is adjusted according to wind intensity and direction ($Wf_{xy,\ i,\ t}$) in relation to neighboring cells that caught fire in time-step $t - 1$ and $Nbf_{xy,\ i,\ t}$, which represents the fire contagion risk from these cells. Risk_TE comes from terrain_effort that describes the effort required for fire to propagate across the landscape dependent upon its direction on the hillside (upslope), plus the presence of physical barriers, so that:

$$\text{terrain\_effort}_{xy,i} = \text{accumuted\_cost\_surface}\ (\text{fland\_cover} + \text{fterrain\_position} + \text{fobstacles})_{xy,i} \quad (2)$$

Firstly, the model assigns a friction value (Table 1) to a cell *xy* according to its relative elevation with respect to immediate neighboring cells that are closer to ignition sources (fterrain_position). Fire spreads more easily outside the forest due to higher flammability of pasture and cropland (fland_cover). High friction values are also assigned to streams (fobstacles), as streams may prevent the direct advance of fire, but not its indirect spread through flying embers. Next, the model calculates a cost-distance map using the friction map and the hot pixels as the source map (Soares-Filho et al. 2010a). Hence, values in the resulting map are proportional to the effort required for the fire to propagate away from its ignition source. Finally, Risk_TE is calculated as follows.

$$\text{Risk\_TE}_{x,y,i} = \frac{e^{W^{+}_{\text{terrain\_effort}_{xy,i}}}}{1 + e^{W^{+}_{\text{terrain\_effort}_{xy,i}}}} \quad (3)$$

where $W^{+}\text{terrain\_effort}_{xy,\ i}$ corresponds to coefficients assigned to ranges of terrain_effort, which were derived by analyzing the spatial dependence between fire scar and cost-distance maps using the weights of evidence method (Soares-Filho et al. 2010a) (Table 1).Favorable climatic conditions for fire spread within the forest (Risk_clim) are a function of IVPD output from CARLUC. Ray et al. (2005) determined that understory fires do not propagate if IVPD is greater than 0.8 kPa in the central-western Amazon. For forests of the Xingu region, we derived a value of 1.3 kPa for this threshold by measuring IVPD around the mapped forest fire scars during the time of their occurrence. Instead of using a binary probability function for fire occurrence, we derived the following equation:

$$\text{Risk\_clim}_{x,y,i} = \text{if deforested then 1 else } \frac{e^{-8.79+6.765*\text{innnerVPD}_{xy,i}}}{1 + e^{-8.79+6.765*\text{innnerVPD}_{xy,i}}} \quad (4)$$

The third component (Risk_Fuel) determines the role of fine litter in inhibiting or facilitating understory fire propagation (Balch et al 2008). This variable is determined using the structural leaf litter pool (StrucLL) simulated within CARLUC. StrucLL is obtained by applying a mortality rate to the leaf pool due to either natural decay or fire event. At each monthly time-step, a fraction of leaves dies naturally as a function of PAW and 90% of the carbon resulting from this process goes to StrucLL (See equation in Fig. 2). According to this equation, a decrease in PAW causes an increase in mortality rates. Hence, as climate becomes drier, the amount of carbon in StrucLL augments, leading to an increase in fuel loads. If a fire event occurs, an additional amount of carbon will be transferred to StrucLL as a result of mortality by fire (Eq. S1, Appendix 6 in Supplementary Material).

Table 1 Model parameter coefficients determined from calibration

Equation no.	Parameter	Description	Value
2	fland_cover	Friction of forest areas, agricultural areas	0.5, 0
2	fobstacles	Friction of streams and water bodies	5
2	fterrain_position	Friction relative to uphill and downhill directions	0.5, 2
3	$W^{+}\text{terrain\_effort}_{xy,\ i}$	Weights of evidence for cost ranges: 0–3, 3–12, 12–15, 15–30, 30–57, 57–60, 60–66, 66–69, 69–105, 105–108, 108–111, 111–114, 114–129, 129–132, 132–258	1.06, 0.73, 0.33, 0.10, −0.07, −0.34, −0.72, −1.44, −1.73, −1.87, −1.93, −2.11, −2.08, −2.08, −2.76
6	τ_wd	Relative azimuth (45° increments)	1.1, 1.05, 1, 0.9, 0.8, 0.9, 1, 1.05
6	*c*	Wind intensity constant	0.06
7	*z*	Constant for number of neighboring cells	0.05

Although fuel load is a determinant of fire risk, field measures of minimum fuel load threshold for a forest to catch fire do not exist for the Amazon. To solve this problem, we constructed a probability function (Eq. 5) and calibrated it so that a 0.5 probability would be expected when fuel loads in StrucLL are around 0.2 kg m^{-2} (figure derived from the percentage of biomass burned), thereby preventing fire recurrence after a sequence of three successive events (Balch et al. 2008).

$$\mathrm{Risk}_{\mathrm{fuel}_{xy,i}} = \frac{e^{-13.05+64.52*\mathrm{strucLL}_{xy,i}}}{1+e^{-13.05+64.52*\mathrm{strucLL}_{xy,i}}} \quad (5)$$

The probabilities of fire from the components Risk_TE, Risk_clim and Risk_fuel are integrated for each cell on a monthly basis after running the ignition source component. Thereafter, the CA module begins by computing the effect of wind intensity and direction from neighboring cells that caught fire in time step $t-1$ on a particular cell so that:

$$\mathrm{Wf}_{xy,i,t} = \tau\_\mathrm{wd}_{x,y,i,t} * e^{C*Wi_{xy,i}} \quad (6)$$

where $wi_{xy,\ i}$ corresponds to the wind intensity in m s^{-1}, c a constant, and $\tau\_\mathrm{wd}_{x,y,i,\ t}$ is the weight for wind direction that is incorporated into the model according to Table 1. Next, the number of neighboring cells burned in step $t-1$ accounts for the probability that a central cell catches fire as follows:

$$\mathrm{Nbf}_{xy,i,t} = (1+zn) \quad (7)$$

where n is the number of adjacent cells—using an 8-cell Moore neighborhood—that burned in a previous step $t-1$, and z is a constant (Table 1). Note that we truncate probabilities greater than 0.9999 in Eq. 1. The CA model iterates 30 times. This number was defined so as to allow fire events to extinguish naturally according to their maximum observed reach across the region's forests: somewhere between 2 and 3 km. In this manner, the model compares the integrated probability of fire (Eq. 1) against a random number generated from a Beta (2.97; 1) distribution in order to stochastically simulate burned cells. The Beta distribution best matched the probability distribution function of cells with fire scars.

The calibration and fine-tuning of model parameters were performed using a genetic algorithm (GA) tool available in Dinamica EGO freeware (Soares-Filho et al. 2010a). We set up the GA tool using k-neighbor estimation, an asymptotic exit condition, and 100 individuals per generation. The GA fitness function compares the match between the number of simulated burned cells with cells with fire scars in 2005 and the proximity of simulated to burned cells determined using the reciprocal fuzzy similarity method (Almeida et al. 2008; Soares-Filho et al. 2010a). Although the model could not be validated with respect to its spatial output patterns due to the absence of time-series of fire scar maps, calibration scores for number of cells burned in 2005 were 100% with spatial accuracy of 50% within a search radius of ~10 km (Fig. S4, Appendix 3 in Supplementary Material).

While the major components of FISC iterate monthly, deforestation and regrowth following land abandonment are simulated on an annual basis. After both components of fire ignition and spread run, the CARLUC model, running at the same spatial resolution of FISC, is called to process interactions between fire and the state of the forest. We initiated CARLUC carbon pools by proportionally rating the equilibrium values with a map of biomass derived from Saatchi et al. (2007)—who estimated that the forests of the Xingu region contain 70 ton ha^{-1} of carbon, on average—in order to reflect current forest carbon content rather than carbon content in a potential equilibrium.

CARLUC includes specific tree mortality rates due to logging and fire events, and therefore explicitly calculates the effects of fire on forest fuel loads and post-fire regeneration (Fig. 2). CARLUC also simulates forest regrowth, which mostly resembles forest recovery after a period of medium-intensity land use (Hirsch et al. 2004). CARLUC was originally developed for the moist forests of Pará. We recalibrated CARLUC to the forests of Xingu by adopting the mortality rates from fire measured in our field experiments at Tanguro (Appendix 6 in Supplementary Material).

Given that estimates of carbon emissions from deforestation vary as a function of the spatial distribution of biomass, land uses, and time following deforestation (Fearnside 1997), we estimated "committed emissions" (Fearnside 1997) assuming that 85% of the carbon contained in forests is released to atmosphere after deforestation (Houghton et al. 2000). In turn, total direct emissions from understory fires are calculated following Balch et al. (2008):

$$\text{Emission\_fire}_i = \sum [\text{CLoss}_{xy,i} * (\text{MetLL}_{xy,i} + \text{StrucLL}_{xy,i}) + 0.44 * \text{Cwd}_{xy,i}] \quad (8)$$

where $\text{CLoss}_{xy,\ i}$ is the combustion percent of the leaf litter pools (Eq. S2, Appendix 6 in Supplementary Material) and $\text{MetLL}_{xy,\ i}$, $\text{StrucLL}_{xy,\ i}$, $\text{Cwd}_{xy,\ i}$ represent the amounts of carbon present in metabolic and structural leaf litter and CWD pools, respectively.

CARLUC, nested in FISC, simulates the interactions between fire and fuel loads; fire-induced leaf mortality transfers carbon to the structural leaf litter and CWD pools, leading, in this case, to an increase in fuel loads. However, fire consumes much more carbon than is replaced by tree mortality. Hence, fuel consumption by a sequence of successive fire events eventually reduces the probability of fire occurring (Balch et al. 2008) until these pools build up again through natural mortality (Fig. 3).

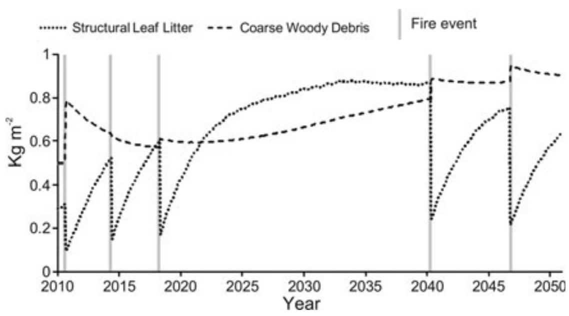

Fig. 3 Interaction between fire and carbon pools of a specific forest location. Structural leaf litter determines the fuel loads and the coarse woody debris pool is where charcoal from fire accumulates

Scenarios of fire, land-cover change and management, and climate change

We ran FISC from 2010 to 2050 under eleven scenarios (Table 2). These scenarios combine the presence and absence of fire with three scenarios of land-cover change, one scenario of climate change versus current conditions and one scenario of fire prevention. The land-cover change scenarios are: (1) the end of deforestation (ED) that assumes an immediate ED (Nepstad et al. 2009) and (2) the business-as-usual (BAU), which assumes the recent deforestation trend (1996–2005 mean annual rate) that resulted from low levels of compliance with environmental laws (Stickler et al. 2009), and (3) the integrated landscape conservation (ILC), which assumes compliance with proposed land-use zoning that includes forest restoration to 50% of private properties in consolidated agricultural zones and reserve compensation between watersheds. In addition, vegetation within 50-m of streams must be strictly protected or restored if absent (Stickler et al. 2009)—Appendix 1 in Supplementary Material. The ILC allows for forest regrowth, and thus presents the greatest extent of forests (secondary plus primary) at the end of the simulation period. Climate scenarios consist of either the impacts of climate change as determined by the HadCM3 model under the SRES-A2 scenario (Cox et al 1999) or the permanence of current climate conditions. Finally, we modeled a better land-use management scenario (BLUM), in which we assume that the effect of Aliança da Terra's Registry of Social-Environmental Responsibility (RSER) and its fire brigades on diminishing the chance of wildfires will be expanded to all

Table 2 Modeled scenarios

	Fire	Land-cover change	Climate change	Fire prevention
NoFire_NoLUC_NoCC	No	No	No	No
NoFire_NoLUC_CC	No	No	Yes	No
Fire_NoLUC_NoCC	Yes	No	No	No
Fire_NoLUC_CC	Yes	No	Yes	No
Fire_LUC_NoCC	Yes	Yes	No	No
Fire_LUC_CC	Yes	Yes	Yes	No
Fire_LUC_NoCC_ILC	Yes	Yes	No	No
Fire_LUC_CC_ILC	Yes	Yes	Yes	No
Fire_NoLUC_NoCC_FP	Yes	No	No	Yes
Fire_LUC_NoCC_ILC_FP	Yes	Yes	No	Yes
Fire_LUC_CC_ILC_FP	Yes	Yes	Yes	Yes

private properties in the Xingu (aliancadaterra.org.br)—Appendix 7 in Supplementary Material.

For each scenario, we analyzed extent of forest burned and total carbon balance of the forest for a 40 year time-period. Since forest extent varies over time in scenarios with land-cover change, we used percentage of forest burned annually instead of total area for comparison. Moreover, because of the historical inhibitory effect of indigenous lands on fire (Nepstad et al. 2006) and of PAs, in general, on deforestation (Soares-Filho et al. 2010b), our analyses are performed separately for areas inside and outside of PAs. Finally, we compared a series of landscape metrics with the extent of forest remnants and percentage of forest burned under BAU (Fire_ LUC_NoCC) to select the metrics that best discern forest fragmentation and its association with fire intensity on the Xingu landscapes (Appendix 8 in Supplementary Material).

Results

The combination of BAU deforestation and climate change (Fire_LUC_CC) indicates the potential for a rampant fire regime across the Xingu landscapes in the near future if common land management practices are maintained. The percentage of forest fragments outside PAs that burn annually increases from the current average of 2.4% to ~10% after 2040, a fourfold increase (Fig. 4). Conversely, the percentage of forest that burns annually inside PAs only increases from 0.2 to 0.3% by midcentury. Under this same scenario, in which deforestation removes 56% of the current forest extent outside PAs by 2050, only 22% of the current forest fragments outside PAs would escape fire or deforestation by 2050, in contrast to 86% of the forest within PAs.

When the effect of climate change is removed from BAU (Fire_LUC_NoCC), the percentage of forest

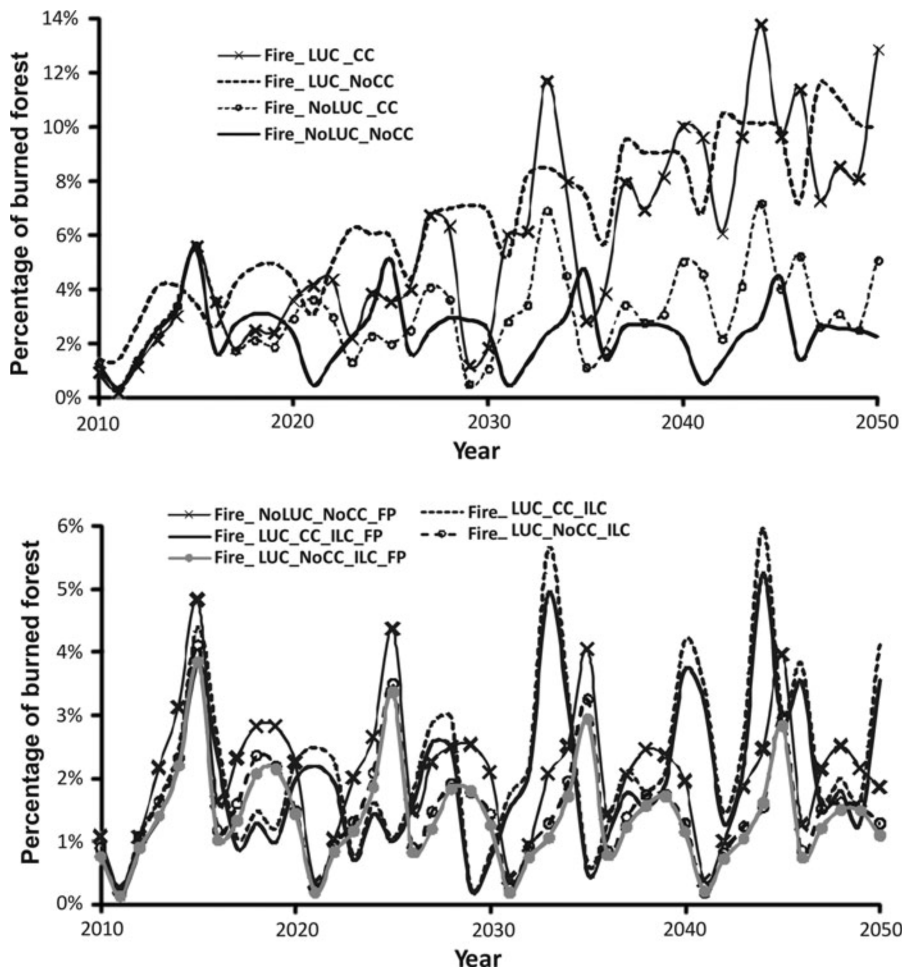

Fig. 4 Percentage of forest burned outside PAs under modeled scenarios

burned outside PAs almost doubles after 2040. If we compare the annual percentage of forest that burns over the 40 years period, BAU in conjunction with climate change may increase the impact of fire on the forest by 140%, or double it if climate change is not considered. Although Fig. 4 does not show seasonal variability, fire activity is, on average, four times more intense during the dry season. The climatic fire risk component of FISC predicts this intra-annual variability well (Fig. S3, Appendix 2 in Supplementary Material).

For the ED scenario, the percentage of forest burned annually after 2040 inside and outside of PAs increases by 68 and 71%, respectively, as a result of climate change (Fire_NoLUC_CC). Therefore, the impact of climate change on fire is considerably less in the absence of continued deforestation and forest fragmentation. In the climate change only scenario (Fire_ NoLUC _CC), understory fires would affect forests outside PAs once every 35 years, on average—a figure 33% higher than the current frequency. Yet only 56% of the forest fragments outside PAs would have escaped fire by 2050, as opposed to 63% under current conditions. The average frequency of understory fires in PAs would be once every 343 years with climate change and once every 495 years under current climate conditions (NoFire_NoLUC_NoCC). In addition, 93–95% of forests within PAs would escape fire by 2050 either under Fire_NoLUC_NoCC or Fire_ NoLUC _CC. Under current conditions, BLUM could reduce current fire activity outside PAs by 13% (Fire_ NoLUC_NoCC_FP), while ILC would abate fire by 36% by midcentury as a result of forest recovery (Fire_ LUC_NoCC_ILC), or 7% if combined with climate change (Fire_ LUC_CC_ILC). Of particular importance, the combination of BLUM and ILC under current climate conditions (Fire_ LUC_ NoCC_ILC_ FP) would abate fire by 42% by midcentury, compared to current regime, or by 18% even in the event of climate change (Fire_ LUC_ CC_ILC_ FP) (Fig. 4).

Of the factors we considered, forest restoration has, therefore, the single largest impact on preventing understory fires in the Xingu region, demonstrating that the major driver of fire in the Xingu headwaters for the next four decades is forest fragmentation rather than climate change. In this regard, we found that a set of metrics representing four of the seven universal landscape structure components—namely dominance of large patches, patch clumpiness, shape variability, and isolation (Cushman et al. 2008)—are well-suited to relate landscape structure and fire. These metrics are, respectively, (1) largest patch index, (2) index of contagion, (3) perimeter to area ratio, and (4) mean patch distance. All these metrics showed high association with extent of forest remnants ($R^2 = 0.88$–0.99) and percentage of forest burned outside PAs ($R^2 = 0.87$–0.99) for the Xingu landscapes (Appendix 8 in Supplementary Material).

With respect to the carbon balance of the region's forests, in the absence of fire, deforestation and climate change (NoFire_NoLUC_NoCC), CARLUC simulates a net balance of 1.6 ± 0.5 ton ha^{-1} year^{-1}, on average (Fig. 5), but varying from 3.5 to a low of 0.5 ton ha^{-1} year^{-1} in drought years (positive sign means carbon removal and negative emissions). The range of these values is in accordance with field measurements in other Amazon regions, especially those situated in the southern Amazon (Philips et al. 2009). This fact supports CARLUC's ability to simulate carbon fluxes between forest pools and from the forest to the atmosphere in the absence of disturbance by fire or logging. Results from CARLUC also show that climate change alone (NoFire_ NoLUC _CC) could reduce total carbon removed from the atmosphere by the forests by 12% over the next four decades. Fire in the ED scenario would diminish the total forest carbon budget by 4% without climate change (Fire_ NoLUC_NoCC) and by 18% with climate change—Fire_ NoLUC _CC (respectively, 1 and 16% within and 6 and 19% outside PAs). Although total direct emissions from understory fires in the Xingu headwaters are around 0.8 Mton year^{-1} in normal years, they can reach up to 2.7 Mton year^{-1} in drought years (Fig. 6), notwithstanding their indirect impact that continues to be large over time due to post-fire forest mortality. Moreover, if emissions from deforestation are added to emissions from fire and reduction of carbon sequestration by climate change, the forest would become a source of carbon over the next four decades with an annual average net balance of—0.1 Mton ha^{-1} year^{-1} (Fire_ LUC _CC). This scenario might be even more dramatic if it weren't for the inhibitory effect of the Xingu Indigenous Park and other PAs on deforestation in the region. However, the effect of fire on the forest carbon balance could be further aggravated as drought events increase in frequency and intensity due to global warming. In

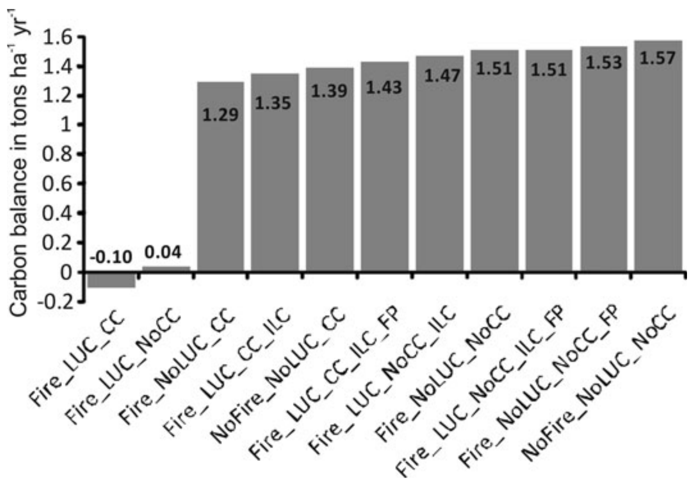

Fig. 5 Annual mean carbon balance for the modeled scenarios

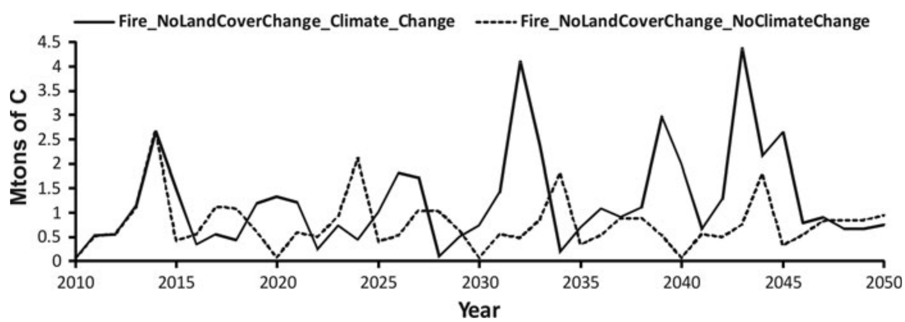

Fig. 6 Forest fire emissions under no deforestation and climate change scenarios (Fire_NoLUC_CC) and no climate change (Fire_NoLUC_NoCC)

fact, our results show that climate change alone (Fire_ NoLUC _CC) would increase fire emissions by 60% over the next 40 years, and boost peak carbon emissions from forest fires in El-Niño-like years by up to 4.3 Mton year^{-1} (Fig. 6). Finally, in the combined BLUM and ILC scenario (Fire_ LUC_NoCC_ILC_FP), better land-use management and forest restoration, which greatly compensates additional deforestation, could sequester 1.51 $\pm$ 0.5 ton ha^{-1} year^{-1} of carbon, on average, over the next 40 years, or 1.43 $\pm$ 0.5 ton ha^{-1} year^{-1} in the event of climate change (Fire_ LUC_CC_ILC_FP) (Fig. 5).

Discussion

Our fire simulations under climate and land-cover scenarios suggest that the major driver of understory fires today and in the near future is forest fragmentation rather than climate change. Nevertheless, better land-use management practices associated with fire prevention and suppression campaigns, if expanded and consolidated throughout the region, could tame wildfires. Understory fire intensity proved to be closely related to a set of landscape metrics that describe the structure of the remaining forest. While climate change may increase the percentage of forest burned outside PAs by 30% over the next four decades, forest fragmentation alone may double it. In addition, synergy between climate change and deforestation could further contribute to fire, increasing the percentage of forest burned outside PAs by 140% over the next four decades. Conversely, the adoption of a conservation and fire prevention scenario (Fire_ LUC_CC_ILC_FP) would abate fire by 18% by midcentury even in the event of climate change.

The extent to which climate change will affect future fire regimes is still uncertain and will depend upon the improvement of global climate models. With this in mind, we used the outputs from the HadCM3 model to set an upper bound for the effects of climate change since this model, although highly ranked among the IPCC models (IPCC 2007), predicts the most severe forest dieback effects in the Amazon (Malhi et al. 2009). Even so, our study shows that forest fragmentation rather than climate change will continue to be the major driver of forest fires in the Amazon. In future FISC runs, this tendency could be balanced by employing projections from other climate models under a broader set of climate scenarios. The prompt availability of climate data in standard GIS format (e.g. Geotiff) will greatly facilitate the utilization of those projections in models that integrate responses of landscape processes to climate change.

In terms of the carbon balance, our results also support those of Philips et al. (2009), who showed that the Amazon forest is sequestering carbon under stable climatic conditions. However, it is clear that as climate change and deforestation are included in simulations, the forest's ability to sequester carbon becomes impaired and may ultimately shift the forest from a net sink to a source of atmospheric CO_2. Regarding our estimates of carbon balance, two sources of uncertainty must be mentioned. Firstly, it is important to stress that the field experiments that provided data for FISC's emission rates (Balch et al. 2008) were conducted in non-logged forests, suggesting that our results might underestimate fire emissions in the case of logged forests, which mostly occur in the northwestern of Xingu. Secondly, recurrent fires also modify forest composition, inducing the spread of pyrophytic vegetation, such as bamboos and grasses (Barlow and Peres 2008). Hence the inclusion of this process would increase forest flammability and also raise our emission estimates.

Our modeled fire results showed large differences inside and outside of PAs, with forests inside PAs much less impacted by climate change. This result is in agreement with previous studies which indicate that preserving large tracts of undisturbed forests is the single most important factor for maintaining the Amazon forest (Cochrane and Barber 2009; Malhi et al 2009).

Conclusion and outlook

Fire modeling provides a unique opportunity to investigate the cornerstone concept of landscape ecology in an integrated fashion, i.e. the interactions between landscape structure, functioning and dynamics and human dimensions (Forman and Godron 1986). In this regard, our model explicitly incorporates better land-use management practices and the spatial patterns resulting from different land-cover scenarios into simulations of tropical forest fire. Hence it can be used as a tool to explore the effects of various land-use practices and forest remnant configurations, including the design of forest corridors, on understory fires, and thus on forest vulnerability. To this end, FISC deals with patch size and form and forest connectivity resulting from multiple transitions between the elements of the landscape (Soares-Filho et al. 2002; 2010a). Additionally, FISC incorporates advances in fire science from field experiments, remote sensing, and global climate models, making it capable of simulating the processes of fire ignition and propagation and the effects of fire on carbon cycling and forest dynamics at a high spatial resolution (<1 km^2). Hence, the FISC framework represents a bottom-up approach that aims to bridge the gap in modeling the feedbacks between climate change, deforestation, logging, and fire in the Amazon (Nepstad el al. 2008).

As a next step, we plan to expand FISC to the entire Amazon and to fully couple it to a dynamic vegetation model capable of running at a high spatial resolution (e.g. Santos and Costa 2004), in order to include feedbacks between fire and changes in vegetation composition. This effort will rely heavily on field measurements of the impacts of fire on other Amazon ecosystems, which are still rare, and the prompt availability of basin-wide time-series maps of forest fire scars (Alencar et al. 2011). These new data will stir up advancements in the science of tropical fire. Still, future availability of land-use maps that differentiate between ranching and crop farming and between large and small landholders will increase accuracy of fire prediction in FISC, given that fire is highly associated with land management practices within a specific set of land-use activities (Alencar et al. 2006), and is less likely in regions with a greater concentration of agro-industrial annual crop production.

Efforts to reduce wildfires must also focus on promoting active fire prevention campaigns, investing in fire brigades, and discouraging land-use management practices commonly associated with fire. These goals could be also accomplished by expanding the number of farms under RSER and strengthening best land-use practices to small landholders through credit mechanisms (Carmenta et al. 2011).

Finally, our results have implications for REDD+, as FISC can estimate carbon emission from forest degradation by fire, the second D of REDD+, as well as enhancement of forest carbon stocks through vegetation regrowth. In this sense, not only do our modeling results confirm the synergy of the two Ds of REDD+, which must indeed be tackled together (Aragão and Shimabokuro 2010), but also point out the co-benefits of REDD+ in maintaining the health of forest ecosystems and hence their resilience in the face of climate change.

Acknowledgments We thank the Gordon and Betty Moore Foundation, the David and Lucille Packard Foundation, Conselho Nacional de Desenvolvimento Científico e Tecnológico, and the Large-Scale Biosphere Atmosphere Experiment for funding. Special thanks go to Jennifer Balch and the field team.

References

Alencar A, Solorzano LA, Nepstad DC (2004) Modeling forest understory fires in an eastern Amazonian landscape. Ecol Appl 14(4):S139–S149

Alencar A, Nepstad DC, Vera Diaz MDC (2006) Forest understory fire in the Brazilian Amazon in ENSO and non ENSO years: area burned and committed carbon emissions. Earth Interact 10:1–16

Alencar A, Asner GP, Knapp D, Zarin D (2011) Temporal variability of forest fires in eastern Amazonia. Ecol Appl 21(7):2397–2412

Almeida CM, Gleriani JM, Castejon EF, Soares-Filho BS (2008) Neural networks and cellular automata for modeling intra-urban land use dynamics. Int J Geogr Inf Sci 22(9):943–963

Aragão LEOC, Shimabokuro YE (2010) The incidence of fire in Amazonian forests with implications for REDD. Science 328:1275–1278

Balch JK, Nepstad DC, Brando PM, Curran LM, Portela O, Carvalho O Jr, Lefebvre P (2008) Negative fire feedback in a transitional forest of Southeastern Amazonia. Glob Change Biol 14:1–12

Barlow J, Peres CA (2008) Fire-mediated dieback and compositional cascade in an Amazonian forest. Philos Trans R Soc B 363(1498):1787–1794

Betts RA, Cox PM, Collins M, Harris PP, Huntingford C, Jones CD (2004) The role of ecosystem-atmosphere interactions in simulated Amazon forest dieback under global climate warming. Theor Appl Climatol 78:157–175

Cardoso MF, Hurtt CG, Moore (2003) Projecting future fire activity in Amazonia. Glob Change Biol 9:656–669

Carmenta R, Parry L, Blackburn A, Vermeylen S, Barlow J (2011) Understanding human-fire interactions in tropical forest regions: a case for interdisciplinary research across the natural and social sciences. Ecol Soc 16(1):53

Cochrane MA (2003) Fire science for rainforests. Nature 421:913–919

Cochrane MA, Barber CP (2009) Climate change, human land use and future fire in the Amazon. Glob Change Biol 15:601–612

Cochrane MA, Alencar A, Shulze MD, Souza CM Jr, Nepstad DC, Lefebvre P, Davidson EA (1999) Positive feedbacks in the fire dynamic of closed canopy tropical forests. Science 284:1832–1835

Collins M, The CMIP Modelling Groups: BMRC (Australia), CCC (Canada), CCSR/NIES (Japan), CERFACS (France), CSIRO (Austraila), MPI (Germany), GFDL (USA), GISS (USA), IAP (China), INM (Russia), LMD (France), MRI (Japan), NCAR (USA), NRL (USA), Hadley Centre (UK), YNU (South Korea) (2005) El Niño- or La Niña-like climate change? Clim Dyn 24:89–104

Cox PM, Betts RA, Bunton CB, Essery RLH, Rowntree PR, Smith J (1999) The impact of new land surface physics on the GCMsimulation of climate and sensitivity. Clim Dyn 15:183–203

Cox PM, Betts RA, Collins M, Harris PP, Huntingford C, Jones CD (2004) Amazonian forest dieback under climate-carbon cycle projections for the 21st century. Theor Appl Climatol 78(1–3):137–156

Cox PM, Harris PH, Huntingford C, Betts RA, Collins M, Jones CD, Jupp TE, Marengo JA, Nobre CA (2008) Increasing risk of Amazonian drought due to decreasing aerosol pollution. Nature 453:212–216

Cushman SA, McGarigal K, Neel MC (2008) Parsimony in landscape metrics: strength, universality, and consistency. Ecol Indic 8:691–703

Fearnside PM (1997) Greenhouse gases emissions from deforestation in Amazonia: net committed emissions. Clim Change 35:321–360

Forman RTT, Godron M (1986) Landscape ecology. Wiley, New York

Green DG (1983) Shapes of simulated fires in discrete fuels. Ecol Model 20:21–32

Hirsch AI, Little WS, Houghton RA, Scott NA, White JD (2004) The net carbon flux due to deforestation and forest regrowth in the Brazilian Amazon: analysis using a process-based model. Glob Change Biol 10:908–924

Houghton RA, Skole DL, Nobre CA, Hackler JL, Lawrence KT, Chomentowski WH (2000) Annual fluxes of carbon from deforestation and regrowth in the Brazilian Amazon. Nature 403:301–304

IPCC (2007) Climate change 2007: The Physical Science Basis. Contribution of Working Group I to the Fourth Assessment Report of the Intergovernmental Panel on Climate Change. Cambridge University Press, Cambridge

Johnstone J, Rupp T, Olson M, Verblya D (2011) Modeling impacts of fire severity on successional trajectories and future fire behavior in Alaskan boreal forests. Landscape Ecol 26:487–500

Kapos V, Ganade G, Matsui E (1993) d13C as an indicator of edge effects in tropical rainforest reserves. J Ecol 81:425–431

Malhi YJ, Aragão LEOC, Galbraith D, Huntingford C, Fisherd R, Zelazowski P, Sitche S, McSweeneya C, Meirb P (2009) Exploring the likelihood and mechanism of a climate-change-induced dieback of the Amazon rainforest. Proc Natl Acad Sci USA 106:20610–20615

Marengo JA, Nobre CA, Tomasela J, Oyama MD, Oliveira GS, Oliveira R, Camargo H, Alves LM, Brown IF (2008) The drought of Amazonia in 2005. J Clim 21:495–516

Melillo JM, McGuire DA, Kicklighter DW, Moore B III, Vorosmarty CJ, Schloss AL (1993) Global climate change and terrestrial net primary production. Nature 363:234–240

Nepstad DC, Verissimo A, Alencar A, Nobre C, Lima E, Lefebvre P, Shlesinger P, Potterk C, Moutinho P, Mendoza E, Cochrane M, Brooksk V (1999) Large-scale impoverishment of Amazonian forests by logging and fire. Nature 398:505–508

Nepstad DC, Lefebvre P, Silva UL, Tomasella J, Schlesinger P, Solórzano L, Moutinho P, Ray D, Benito JG (2004) Amazon drought and its implications for forest flammability and tree growth: a basin wide analysis. Glob Change Biol 10:1–14

Nepstad DC, Shwartzman S, Bamberger B, Santilli M, Ray D, Schlesinger P, Lefebvre P, Alencar A, Prinz E, Fiske G, Rolla A (2006) Inhibition of Amazon deforestation and fire by parks and indigeous Lands. Conserv Biol 20:65–73

Nepstad DC, Stickler C, Soares Filho BS, Merry F (2008) Interactions among Amazon land use, forests, and climate: prospects for a near-term forest tipping point. Philos Trans R Soc B 363(1498):1737–1746

Nepstad D, Soares-Filho BS, Merry F, Lima A, Moutinho P, Carter J, Bowman M, Cattaneo A, Rodrigues H, Schwartzman S, McGrath DG, Stickler CM, Lubowski R, Piris-Cabezas P, Rivero S, Alencar A, Almeida O, Stella O (2009) The end of deforestation in the Brazilian Amazon. Science 326:1350–1351

Oyama MD, Nobre CA (2003) A new climate-vegetation equilibrium state for Tropical South America. Geophys Res Lett 30(23):2199. doi:10.1029/2003GL018600.2003

Phillips OL, Aragão LEOC, Lewis SL, Fisher JB, Lloyd J, López-González G, Malhi Y, Monteagudo A, Peacock J, Quesada CA, Heijden G, Almeida S, Amaral I, Arroyo L, Aymard G, Baker TR, Bánki O, Blanc L, Bonal D, Brando P, Chave J, Oliveira ACA, Cardozo ND, Czimczik CI, Feldpausch TR, Freitas MA, Gloor E, Higuchi N, Jiménez E, Lloyd G, Meir P, Mendoza C, Morel A, Neill DA, Nepstad D, Patiño S, Peñuela MC, Prieto A, Ramírez F, Schwarz M, Silva J, Silveira M, Thomas AS, Steege H, Stropp J, Vásquez R, Zelazowski P, Dávila EA, Andelman S, Andrade A, Chao KJ, Erwin T, Di Fiore A, Honorio E, Keeling H, Killeen TJ, Laurance WF, Cruz AP, Pitman NCA, Vargas PN, Ramírez-Ângulo H, Rudas A, Salamão R, Silva N, Terborgh J, Torres-Lezama A (2009) Drought sensitivity of the Amazon rainforest. Science 323:1345–1347

Phulpin T, Lavenu F, Bellan MF, Mougenot B, Blasco F (2002) Using SPOT-4 HRVIR and vegetation sensors to assess impact of tropical forest fires in Roraima, Brazil. Int J Remote Sens 23:1943–1966

Ramming A, Jupp T, Thonicke K, Tietjen B, Heinke J, Ostberg S, Lucht W, Cramer W, Cox P (2010) Estimating the risk of Amazonian forest dieback. New Phytol 87(3):694–706

Ray D, Nepstad D, Moutinho P (2005) Micrometeorological and canopy controls of fire susceptibility in forested Amazon landscape. Ecol Appl 15:1664–1678

Saatchi SS, Houghton RA, Alvalá RCS, Soares JV, Yu Y (2007) Distribution of aboveground live biomass in the Amazon Basin. Glob Change Biol 13:816–837

Sampaio G, Nobre C, Costa MH, Satyamurty P, Soares-Filho BS, Cardoso M (2007) Regional climate change over eastern Amazonia caused by pasture and soybean cropland expansion. Geophys Res Lett 34(17):L17709. doi:10.1029/2007GL030612

Santos SNM, Costa MH (2004) A simple tropical ecosystem model of carbon, water and energy fluxes. Ecol Model 176:291–312

Silvestrini RA, Soares-Filho BS, Nepstad D, Coe M, Rodrigues HO, Assunção R (2011) Simulating fire regimes in the Amazon in response to climate change and deforestation. Ecol Appl 21(5):1573–1590

Sismanoglu RA, Setzer AW (2005) Risco de fogo da vegetação na América do Sul: comparação de três versões na estiagem de 2004. Paper presented at the XII Simpósio Brasileiro de Sensoriamento Remoto, Goiania, Brazil, 16–21 Apr 2005

Soares Filho BS, Pennachin CL, Cerqueira G (2002) DINAMICA—a stochastic cellular automata model designed to simulate the landscape dynamics in an Amazonian colonization frontier. Ecol Model 154(3):217–235

Soares-Filho BS, Nepstad DC, Curran LM, Cerqueira GC, Garcia RA, Ramos CA, Voll E, McDonald A, Lefebvre P, Schlesinger P (2006) Modelling conservation in the Amazon basin. Nature 440(7083):520–523

Soares-Filho BS, Rodrigues HO, Costa WL (2010a) Modeling environmental dynamics with dinamica EGO. Centro de Sensoriamento Remoto, Belo Horizonte, Brazil. http://www.csr.ufmg.br/dinamica. Accessed May 2010

Soares-Filho BS, Moutinho P, Nepstad D, Anderson A, Rodrigues H, Garcia R, Dietzsch L, Merry F, Bowman M, Hissa L, Silvestrini R, Maretti C (2010b) Role of Brazilian Amazon protected areas in climate change mitigation. Proc Natl Acad Sci USA 107(24):10821–10826

Stickler CM, Nepstad DC, Coe MT, Mcgrath DG, Rodrigues HO, Walker WS, Soares-Filho BS, Davidson EA (2009) The potential ecological costs and co-benefits of REDD: a critical review and case study from the Amazon region. Glob Change Biol 15:2803–2824

Turner MG, Romme WH (1994) Landscape dynamics in crown fire ecosystems. Landscape Ecol 9:59–77

Van der Werf GR, Morton DC, DeFries RS, Giglio L, Randerson JT, Collatz GJ, Kasibhatla PS (2009) Estimates of fire emissions from an active deforestation region in the southern Amazon based on satellite data and biogeochemical modelling. Biogeosciences 6:235–249

World Bank (2010) Assessment of the risk of Amazon dieback Main Report. World Bank, Climate Change and Clean Energy Initiative, Environmentally and Socially Sustainable Development Department, Latin America and Caribbean Region. http://www.bicusa.org/en/Document.101982.aspx. Accessed October 2011